THE JOURNAL OF BIOLOGICAL CHEMISTRY VOL. 282, NO. 16, pp. 11931–11940, April 20, 2007


# Hsp40 Interacts Directly with the Native State of the Yeast Prion Protein Ure2 and Inhibits Formation of Amyloid-like Fibrils*[S]

Received for publication, July 19, 2006, and in revised form, January 16, 2007 Published, JBC Papers in Press, February 26, 2007, DOI 10.1074/jbc.M606856200

**Hui-Yong Lian[‡§], Hong Zhang[‡§], Zai-Rong Zhang[‡§], Harriët M. Loovers[¶], Gary W. Jones[¶1], Pamela J. E. Rowling[‖], Laura S. Itzhaki[‖], Jun-Mei Zhou[‡], and Sarah Perrett[‡2]**

*From the [‡]National Laboratory of Biomacromolecules, Institute of Biophysics, Chinese Academy of Sciences, 15 Datun Road, Chaoyang District, Beijing 100101, China, the [¶]Department of Biology, National University of Ireland Maynooth, Maynooth, Ireland, the [‖]Medical Research Council Cancer Cell Unit, Hutchison/Medical Research Council Research Centre, Hills Road, Cambridge CB2 0XZ, United Kingdom, and the [§]Graduate School of the Chinese Academy of Sciences, Beijing 100039, China*

**Ure2 is the protein determinant of the [*URE3*] prion phenotype in *Saccharomyces cerevisiae* and consists of a flexible N-terminal prion-determining domain and a globular C-terminal glutathione transferase-like domain. Overexpression of the type I Hsp40 member Ydj1 in yeast cells has been found to result in the loss of [*URE3*]. However, the mechanism of prion curing by Ydj1 remains unclear. Here we tested the effect of overexpression of Hsp40 members Ydj1, Sis1, and Apj1 and also Hsp70 co-chaperones Cpr7, Cns1, Sti1, and Fes1 *in vivo* and found that only Ydj1 showed a strong curing effect on [*URE3*]. We also investigated the interaction of Ydj1 with Ure2 *in vitro*. We found that Ydj1 was able to suppress formation of amyloid-like fibrils of Ure2 by delaying the process of fibril formation, as monitored by thioflavin T binding and atomic force microscopy imaging. Controls using bovine serum albumin, Sis1, or the human Hsp40 homologues Hdj1 or Hdj2 showed no significant inhibitory effect. Ydj1 was only effective when added during the lag phase of fibril formation, suggesting that it interacts with Ure2 at an early stage in fibril formation and delays the nucleation process. Using surface plasmon resonance and size exclusion chromatography, we demonstrated a direct interaction between Ydj1 and both wild type and N-terminally truncated Ure2. In contrast, Hdj2, which did not suppress fibril formation, did not show this interaction. The results suggest that Ydj1 inhibits Ure2 fibril formation by binding to the native state of Ure2, thus delaying the onset of oligomerization.**

The epigenetic factor [*URE3*] in the yeast *Saccharomyces cerevisiae* represents the prion form of the protein Ure2 (1). Like the mammalian prion, the heritable [*URE3*] phenotype is conveyed by a structural change in its protein determinant to an aggregated form (1, 2). Ure2 is a 354-amino acid homodimeric protein consisting of a relatively flexible and protease-sensitive N-terminal region (~90 amino acids) and a globular C-terminal region (3–5). The N-terminal region is required for its prion properties *in vivo* (2) and to form amyloid-like filaments *in vitro* (6–8). However, deletion of the N-terminal region has no detectable effect on the stability or folding of the protein *in vitro* (9). The C-terminal region, for which the crystal structure has been determined in both apo (5, 10) and glutathione-bound (11) forms, shows structural similarity to glutathione transferases (GSTs),[3] and is necessary and sufficient for its regulatory function *in vivo*: Ure2 interacts with the transcription factor Gln3, allowing control of nitrogen catabolite repression and blocking the uptake of poor nitrogen sources in the presence of a good nitrogen source (12, 13). In addition, Ure2 possesses glutathione-dependent peroxidase (GPx) activity, which is maintained upon formation of fibrillar aggregates, indicating that the C-terminal globular domains of Ure2 retain their native structure within the fibrils (14).

Ydj1 from *S. cerevisiae* is a molecular chaperone of the type I Hsp40 family and is involved in multiple functions, including import of proteins into mitochondria, secretion of mating pheromones, and regulation of the activity of the cytoplasmic Hsp70s (15–17). Ydj1 can bind to nonnative polypeptides and pair with Hsp70 Ssa proteins to prevent aggregation and facilitate refolding of denatured proteins *in vitro* (18–20). In contrast to Sis1 (a type II Hsp40 from *S. cerevisiae*), Ydj1 itself can act as a chaperone *in vitro*, suppressing protein aggregation by forming stable complexes with folding intermediates (18, 19).

Like other heat-shock proteins (21), Hsp40 members have been found to play a role in yeast prion propagation. Overexpression of Ydj1 results in the loss of the [*URE3*] phenotype (22)

* This work was supported by Natural Science Foundation of China Grants 30470363, 30620130109, and 30670428; Chinese Ministry of Science and Technology Grants 2006CB500703 and 2006CB910903; Chinese Academy of Sciences Knowledge Innovation Project Grant KSCX2-SW214-3; and core funding from the Institute of Biophysics (to S. P.). Work performed in the Itzhaki laboratory was supported by the Medical Research Council (to L. S. I.) and by a European Molecular Biology Organization short term fellowship (to S. P.). Exchange between the Jones and Perrett laboratories was supported by China/Ireland Science and Technology Collaboration Research Fund Grant CI-2004-01. The costs of publication of this article were defrayed in part by the payment of page charges. This article must therefore be hereby marked "*advertisement*" in accordance with 18 U.S.C. Section 1734 solely to indicate this fact.

[S] The on-line version of this article (available at http://www.jbc.org) contains supplemental Fig. S1.

[1] Supported by the Irish Health Research Board.

[2] To whom correspondence should be addressed. Tel.: 86-10-6485-6727; Fax: 86-10-6487-2026; E-mail: sarah.perrett@iname.com.

[3] The abbreviations used are: GST, glutathione *S*-transferase; 90Ure2, Ure2 lacking residues 1–89 of the N-terminal prion domain; 105Ure2, Ure2 lacking the entire unstructured N-terminal region; AFM, atomic force microscopy; GPx, glutathione peroxidase; Hsp, heat shock protein; SPR, surface plasmon resonance; ThT, thioflavin T; WT, wild type.

and also cures certain variants of another yeast prion [*PIN*$^+$]/[*RNQ*$^+$] (23). Overexpression of Sis1 is unable to cure [*RNQ*$^+$] (24). [*RNQ*$^+$] interacts with both Sis1 and Ydj1, and Sis1 is required for maintenance of [*RNQ*$^+$], suggesting that the curing effect of Ydj1 may interfere with the role of Sis1 in maintenance (25, 26). Weak strains of [*PSI*$^+$] can be cured by Ydj1 only when Ssa1 is also overexpressed (27). *In vitro*, fibril formation of the [*PSI*$^+$] determinant Sup35 was clearly reduced in the presence of the combination of Ssa1 and either Ydj1 or Sis1; Ydj1 (but not Sis1) alone also showed a moderate reduction (28). Co-chaperones containing the tetratricopeptide repeat motif, such as Sti1, Cpr7, and Cns1; the nucleotide exchange factor Fes1; and Hsp40 members Ydj1 and Sis1 have all been implicated in propagation of [*PSI*$^+$] through an Hsp70-dependent mechanism (reviewed in Ref. 21). Apj1, a putative Type I Hsp40 member, was found to cure an artificial variant of [*PSI*$^+$] (29). In the case of [*URE3*], besides Ydj1, overexpression of the Hsp70 protein Ssa1 also cures [*URE3*] (30), and a mutation in the peptide-binding domain of its closely related homologue Ssa2 abolishes [*URE3*] propagation (31). In addition, mutants in the ATP-binding domain of both Ssa1 and Ssa2 are found to affect [*URE3*] propagation (32). Hsp104 is required for maintenance of [*URE3*] (22), as found for other yeast prions (21). Since Ydj1 stimulates the ATPase activity of Ssa1/Ssa2 (18, 33) and also cooperates with Hsp70 and Hsp104 in protein disaggregation (34), it cannot be deduced from the current genetic data whether [*URE3*] curing by Ydj1 reflects increased stimulation of Hsp70 activity or directly reflects the chaperoning properties of Ydj1 itself.

In order to address this question, we examined the effect of overexpressing a variety of Hsp70 co-chaperones on curing of [*URE3*] *in vivo* and investigated the effect of Hsp40 on fibril formation of Ure2 *in vitro*. The results imply a direct and specific effect of Ydj1 on [*URE3*] propagation and suggest that Ydj1 inhibits Ure2 fibril formation by binding to the native state of Ure2, prior to the onset of oligomerization.

## EXPERIMENTAL PROCEDURES

*Materials*—Tris, sodium azide, GSH, β-NADPH, cumene hydroperoxide, and thioflavin T (ThT) were from Sigma. All other reagents were local products of analytical grade. Twice-deionized water was used throughout. Solutions were made volumetrically.

*Yeast Strains, Plasmids, and Genetic Methods*—Strain NT64C (*MAT***a**, *ade2-1*, *his3-11,15*, *leu2*, *3-112*, *trp1-1*, *ura3,1*, *pDAL5*::*ADE2*, [*URE3*]; constructed by L. Ripaud and a gift from C. Cullin) was used for assessment of *in vivo* co-chaperone effects on [*URE3*] propagation. Plasmids overexpressing co-chaperones were constructed by PCR amplification of target gene coding sequence ±500 bp using primers containing BamHI restriction sites at their ends. Following digestion with BamHI, PCR products were cloned into the unique BamHI site of the high copy *HIS3*-based plasmid pRS423 (35). Co-chaperones chosen for analysis were *YDJ1*, *SIS1*, *APJ1*, *CPR7*, *CNS1*, *STI1*, and *FES1*. All plasmids were verified by sequencing. Assessment of effects of co-chaperone overexpression on [*URE3*] propagation was carried out by transforming NT64C with the desired co-chaperones cloned into pRS423. Transformants were selected on medium lacking histidine. NT64C contains the *DAL5* promoter sequence cloned upstream of the *ADE2* coding region and allows identification of [*URE3*] and [*ure-0*] cells initially by color: white and red, respectively. White *HIS3*$^+$ transformants were selected and restreaked onto medium lacking histidine to assess color phenotype. Plates were incubated for 2 days at 30 °C and a further 2 days at room temperature. The presence of red or pink colonies is indicative of a curing effect on propagation of [*URE3*].

*Protein Preparation*—Ydj1 and Hsp104 were subcloned from plasmids provided by Dr. D. C. Masison and ligated into the vector mini-pRSETa (provided by Dr. M. Bycroft). The Ydj1 plasmid was then transformed into *Escherichia coli* strain C41 (36). The cells were incubated at 37 °C and induced by the addition of 100 μM isopropyl 1-thio-β-D-galactopyranoside when the OD at 600 nm reached 0.5–0.8. The cells were grown for a further 12 h before harvesting and lysis by sonication. The expressed protein with an N-terminal $His_6$ tag was purified using $Ni^{2+}$ affinity chromatography and was judged greater than 90% pure by SDS-PAGE. The protein was confirmed to be dimeric by size exclusion chromatography. The Sis1 expression plasmid was a gift from Dr. Stefan Walter. Hdj1 and Hdj2 were subcloned from plasmids provided by Prof. R. Morimoto into the expression system used for Ydj1. Sis1, Hdj1, Hdj2, and Hsp104 were expressed and purified in the same way as Ydj1. Ydj1, Sis1, Hdj1, Hdj2, and Hsp104 with N-terminal His tags have been shown to be functional *in vivo* (19, 37) and/or *in vitro* (19, 20, 37–40), so in general the His-tagged proteins were used. Alternatively, the His tag was cleaved from Ydj1 using thrombin, and the protein was further purified by gel filtration. Reducing agents, such as dithiothreitol or β-mercaptoethanol, were omitted, since these were found in control experiments to stimulate fibril formation of Ure2, and their inclusion would therefore complicate interpretation of the results. (The mechanism of this is currently under investigation.) Wild type Ure2 and its mutants were produced with an N-terminal His tag and purified under native conditions as described (3, 41).

All protein concentrations (in terms of monomers) were measured by absorbance at 280 nm using the calculated extinction coefficient (42). The mutant 90Ure2 lacks the entire repetitive sequence region (residues 1–89) of the N-terminal prion domain (3), whereas 105Ure2 lacks the entire N-terminal unstructured region (residues 1–104) (9). Both mutants are dimeric, and their stability and folding properties are identical to WT Ure2 (3, 9, 43). All proteins were stored at −80 °C in 50 mM Tris-HCl buffer, pH 7.5, containing 0.2 M NaCl (Buffer A) and defrosted in a 25 °C water bath immediately prior to use. (The stated pH of buffers is correct at 25 °C.)

*In Vitro Amyloid Fibril Formation*—Amyloid formation of Ure2 was performed at 37 °C in Buffer A or in 50 mM sodium phosphate buffer, pH 7.5, containing 0.2 M NaCl (Buffer B), with shaking, essentially as described previously (41), except that shaking was at 230 rpm instead of 200 rpm. These conditions were adopted as standard, because they have been characterized in detail previously (8). However, other conditions of temperature (4, 10, 25, and 30 °C), pH (8.0 and 8.4), and shaking speed (including no agitation) were also tested (see "Results"). The extent of Ure2 fibril formation was monitored by assay of

ThT binding, as described (8, 41). The observed kinetics are sensitive to fluctuations in temperature and shaking speed. Therefore, samples were incubated in parallel, with several replicates for each sample. The results of replicate samples were averaged, and the S.E. was calculated, to confirm that apparent differences were significant. Each experiment was also repeated independently in order to confirm that the observed effects were reproducible.

*Atomic Force Microscopy*—Atomic force microscopy (AFM) was used to analyze the change in morphology of Ure2 aggregates over time in the presence or absence of Ydj1 and was carried out essentially as described (8). Samples were prepared for AFM analysis by spotting 10 $\mu$l of solution onto freshly cleaved mica. Protein was allowed to adhere to the surface for 5 min in air, and then the surface was washed twice with double-distilled $H_2O$ to remove salts before drying for 4 min in a stream of nitrogen. Captured images were obtained using tapping mode with a Nanoscope IIIa Multimode-AFM (Veeco Instruments) under ambient conditions. Super sharp silicon tips (Rtesp; Veeco Instruments) with resonance frequency of about 250 kHz were used at a scan rate of 1–2 Hz. Once the tip was engaged, the set point value was adjusted to minimize the force exerted on the sample while maintaining the sharpness of the image. Samples were imaged at scan sizes between 1 and 10 $\mu$m using line scan rates below 2 Hz, and 512 $\times$ 512 pixels were collected per image.

Height measurements of aggregates and fibrils were performed manually using the software provided with the Nanoscope instrument. The numbers of fibrils and aggregates were counted, and the areas of large aggregates were calculated. In order to ensure that the results were representative, we scanned at least 10 well separated regions of the mica grid for each sample, and we found that the distribution of particles or fibrils was uniform.

*Assay of Ure2 GPx Activity*—The GPx activity of Ure2 and 90Ure2 (final concentration 1.5 $\mu$M) was measured in the presence and absence of Ydj1 at 25 °C in Buffer A, using 1.0 mM GSH and 1.2 mM cumene hydroperoxide as substrates, as described (14). 30 $\mu$M Ure2 was preincubated with or without an equal concentration of Ydj1 for at least 15 min before measuring activity.

*Circular Dichroism*—Spectra were recorded over the range 200–250 nm in a Pistar-180 Spectrometer (Applied Photophysics). Spectra of 20 $\mu$M native Ure2 (or 90Ure2), Ydj1, and their mixture were measured at 37 °C in Buffer A in a 0.1-mm path length thermostatted cuvette after preincubation for 1 h at 37 °C. Spectra of soluble oligomers or complexes formed during the lag time and throughout the time course of fibril formation were also monitored by incubating a series of duplicate samples with and without Ydj1 at 37 °C as for ThT experiments. Samples were removed at a series of time intervals and centrifuged at 18,000 $\times$ *g* for 30 min to remove large aggregates, and then spectra were acquired.

*Analytical Size Exclusion Chromatography*—Size exclusion chromatography experiments were performed at room temperature using a Superdex 200 10/300 GL column equilibrated in Buffer A. 10 $\mu$M samples of WT or N-terminally truncated Ure2 (*i.e.* 90Ure2 or 105Ure2) were preincubated for 15 min with a 1:1 mixture of chaperone before injection and then run at a flow rate of 0.5 ml/min using an AKTA fast protein liquid chromatography system (Amersham Biosciences).

*Surface Plasmon Resonance*—All of the surface plasmon resonance (SPR) experiments were performed on a Biacore X instrument, at 25 °C. The instrument, chips, and buffers were from Biacore Ltd. After optimizing the immobilization conditions on the system check chip, 100 $\mu$g/ml Ure2 in pH 4.5 buffer and 40 $\mu$g/ml 90Ure2 in pH 4.0 buffer were ultimately immobilized onto CM5 chips via amine coupling, giving relative response values of 6454 and 6646, respectively. The control panel was left blank. Binding experiments were performed at a flow rate of 10 $\mu$l/min, using Hepes running buffer HBS-P (10 mM Hepes, pH 7.4, 150 mM NaCl, 0.005% surfactant P20). Protein solutions at different concentrations were perfused over the sensor chip surfaces for 60 s to obtain real time binding data, followed by a 120-s dissociation phase, in order to obtain association ($k_a$) and dissociation ($k_d$) constants. The multichannel detection mode was used to subtract the signal in the reference cell. The surface was regenerated by washing with 1 M NaCl, 100 mM $NaHCO_3$, pH 9.2, and 200 mM $Na_2CO_3$, pH 11.5. Data fitting was performed using the software provided with the instrument, using increasingly complex models until a satisfactory fit of the data was obtained.

## RESULTS

*In Vivo Effects of Co-chaperone Overexpression on [URE3] Propagation*—Previous studies have shown that Hsp70 co-chaperones can have effects on yeast prion propagation and that these effects may be specific to the type of prion being studied (reviewed in Ref. 21). We therefore set out to test, under a single set of experimental conditions, whether overexpression of these various Hsp70 co-chaperones had effects on [*URE3*] propagation.

Fig. 1 shows the effect on [*URE3*] propagation of overexpression of an array of different Hsp40s and known Hsp70 co-chaperones. Using the NT64C strain allows for assessment of [*URE3*] status by color assay. Ure2, in its soluble functional form, binds the transcription factor Gln3, preventing induction of the *DAL5* promoter. Hence, the downstream *ADE2* gene is not expressed, and the result is red-pigmented cells due to the accumulation of an intermediate in the purine biosynthesis pathway, which is the substrate of Ade2 (44). When Ure2 is in the [*URE3*] prion state, functional binding to Gln3 is lost, allowing expression of *ADE2* under control of the *DAL5* promoter. The red pigment is metabolized by Ade2, so it no longer accumulates; hence [*URE3*] cells are white. The presence of a high copy plasmid overexpressing Ydj1 had a clear effect on [*URE3*] propagation, as is reflected by the appearance of red and pink colonies, indicating curing of the prion. Moreover, introduction of an extra single copy of *YDJ1* on a centromeric plasmid is enough to produce a significant number of [*ure-0*] cells in the NT64C strain (data not shown). These results highlight the importance of Ydj1 compared with the other co-chaperones we tested in the propagation of [*URE3*] *in vivo* and suggest that the curing effect we observe for Ydj1 may be independent of Hsp70.

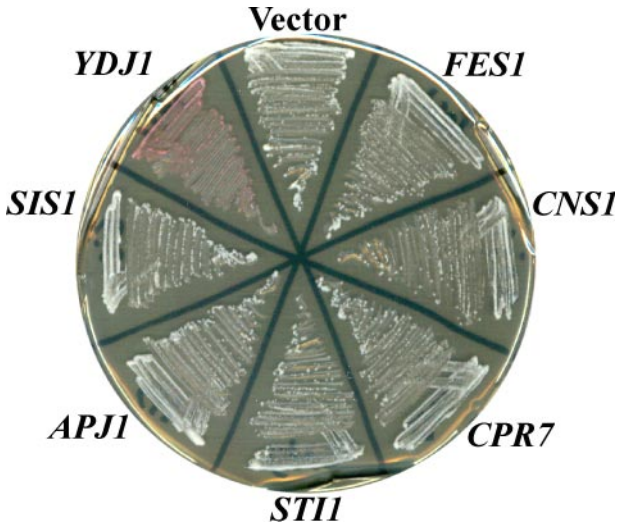


FIGURE 1. **Effects of overexpression of Hsp70 co-chaperones on [*URE3*] propagation.** Strain NT64C was transformed with high copy plasmid expressing the Hsp70 co-chaperones *YDJ1*, *SIS1*, *APJ1*, *CPR7*, *CNS1*, *STI1*, or *FES1*. Shown are *white* NT64C [*URE3*] transformants restreaked onto medium lacking histidine to assess color phenotype. *Red* or *pink* cells, indicating prion curing, were only ever observed at a reproducible high frequency from cells overexpressing *YDJ1*.

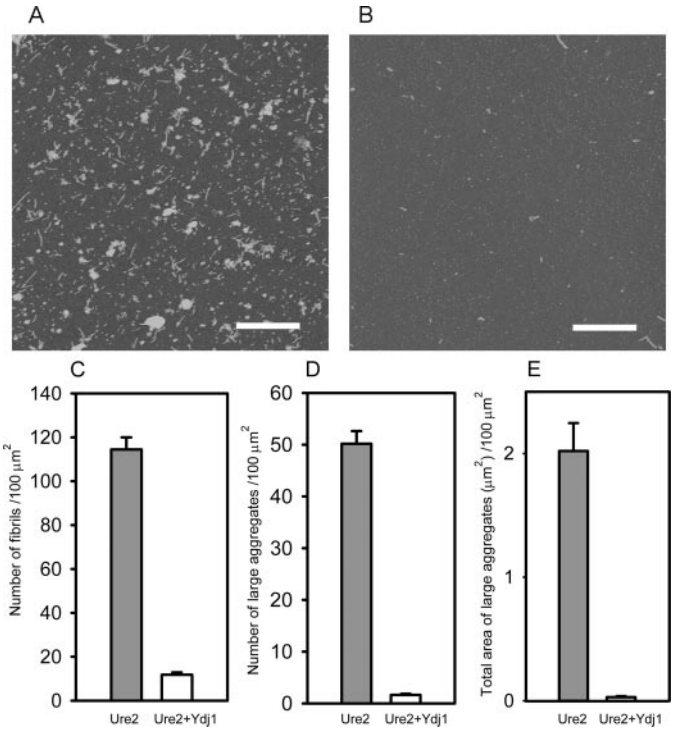


FIGURE 2. **Ydj1 inhibition of Ure2 fibril formation, monitored by AFM.** Conditions were as follows: 50 mM sodium phosphate buffer, pH 7.5, containing 0.2 M NaCl with shaking at 37 °C. The concentration of Ure2 (and Ydj1 if present) was 30 $\mu$M. At least 10 well separated 10 × 10-$\mu$m square scan areas of 15th h samples (plateau phase) were randomly selected for analysis. Representative scan areas are shown for Ure2 alone (*A*) and Ure2 with Ydj1 (*B*). The *scale bar* represents 2 $\mu$m, and the full range of the *gray scale* corresponding to height was 50 nm. The number of fibrils (*C*), number of large aggregates (*D*), and total area of large aggregates (*E*) in the absence (*solid bars*) and presence (*empty bars*) of Ydj1 were calculated manually for these scan areas, and the results were averaged. The *error bars* show the S.E. Aggregates with height 20 nm greater than background were considered as large aggregates.

*The Presence of Ydj1 Inhibits Formation of Ure2 Fibrils and Globular Aggregates in Vitro*—Ure2 forms amyloid-like fibrils *in vitro* (4, 6). Using AFM, a variety of globular and fibrillar species have been observed during the time course of fibril formation (8, 45, 46). AFM was used to monitor the morphology of aggregates generated by Ure2 in both the presence and absence of Ydj1. The various heights of aggregates are represented by a gray scale, ranging from white (high) to black (low), to form the image. Ure2 (30 $\mu$M) was incubated in the presence or absence of an equimolar concentration of Ydj1 for 15 h, which under these conditions is equivalent to the plateau region in the time course of fibril formation (8). Representative AFM images in the absence (Fig. 2*A*) and presence (Fig. 2*B*) of Ydj1 are shown. To ensure that the areas we sampled were indeed representative for the entire sample, we scanned at least 10 areas of fixed size (10 × 10 $\mu$m) on each mica surface. We then counted the number of aggregate particles in each of these AFM images; the averaged results for the number of fibrils (Fig. 2*C*), number of large aggregates (Fig. 2*D*), and area occupied by large aggregates (Fig. 2*E*), per scan area are shown. AFM of Ure2 aggregates in the absence of Ydj1 revealed the presence of many fibrils with a diameter of 9–18 nm and some large globular aggregates with a height (*i.e.* diameter) of at least 20 nm (Fig. 2, *A*, *C*, *D*, and *E*). When Ydj1 was included in the incubation reaction, relatively few fibrils were observed, and large aggregates were rarely seen (Fig. 2, *B*–*E*). These results indicate that an equimolar concentration of Ydj1 suppresses the formation of globular and fibrillar aggregates of Ure2.

*The Presence of Ydj1 Delays Formation of Amyloid-like Structure in Ure2*—In order to investigate the effect of Ydj1 on the kinetics of fibril formation, we used binding of the fluorescence dye ThT, which is a convenient method to monitor the effect of various factors on the time course of formation of amyloid structure (47, 48), including for Ure2 (41, 49). A sigmoidal time course is observed, with an initial lag phase, followed by an exponential growth phase during which the ThT fluorescence increases and then a plateau. Importantly, the increase in ThT fluorescence has been shown to correlate directly with the appearance of fibrillar aggregates of Ure2, as observed by AFM (8). We therefore used ThT binding to monitor the fibril formation kinetics of a fixed concentration of Ure2 in the presence and absence of various concentrations of Ydj1 to give Ydj1/Ure2 ratios between 0.1 and 5. (The ratio of Ydj1/Ure2 in the cell is reported to be 17:1 (50); however, 5:1 was the highest ratio that could be achieved under the constraints of this experiment.) We found that the presence of Ydj1 reduced the accumulation of ThT-reactive material and increased the lag time in a concentration-dependent manner (Fig. 3, *A* and *B*). Consistent with the AFM result (Fig. 2), when the concentration of Ydj1 was equal to (or greater than) Ure2, there was clear inhibition of amyloid formation. However, when the molar ratio of Ydj1/Ure2 was reduced to 1:3 or below (Fig. 3*A*), the effect of Ydj1 was relatively weak, indicating that Ydj1 inhibits fibril formation in a stoichiometric (rather than a catalytic) manner.

As controls, the presence of an equimolar concentration of bovine serum albumin had no inhibitory effect on Ure2 fibril formation (Fig. 3*C*), indicating that the interaction with Ydj1 is specific, and Ydj1 incubated on its own under the same conditions showed no change in ThT binding fluorescence (Fig. 3*A*). His-tagged Ydj1 (Fig. 3*A*) behaved in the same way as untagged

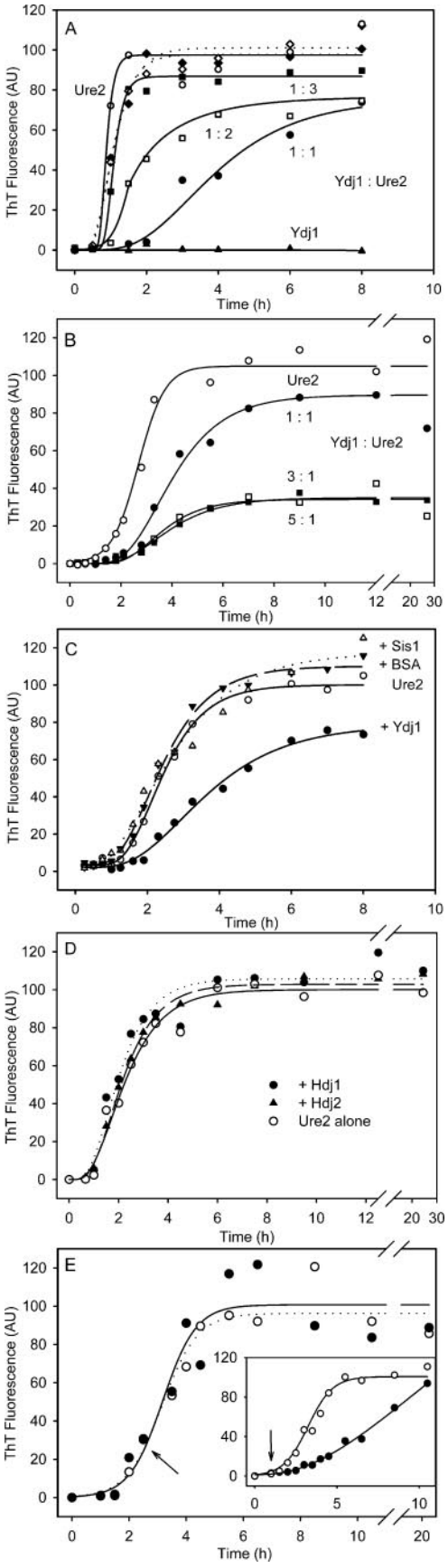


FIGURE 3. **Ydj1 concentration-dependent inhibition of Ure2 fibril formation, monitored by ThT binding.** Conditions were 50 mM Tris-HCl buffer, pH 7.5, containing 0.2 M NaCl with shaking at 37 °C. *A*, fibril formation of 30 $\mu$M Ure2 in the absence (○) and presence of Ydj1 (◇, 3 $\mu$M; ◆, 7.5 $\mu$M; ■, 10 $\mu$M; □, 15 $\mu$M; ●, 30 $\mu$M). As a control, 30 $\mu$M Ydj1 alone (▲) was incubated under the same conditions. (The Ydj1 contained an N-terminal $His_6$ tag.) *B*, fibril formation of 20 $\mu$M Ure2 in the absence (○) and presence of Ydj1 (●, 20 $\mu$M; ■, 60 $\mu$M; □, 100 $\mu$M). *C*, fibril formation of 20 $\mu$M Ure2 alone (○) or in the presence of 20 $\mu$M Ydj1 (●), 20 $\mu$M Sis1 (△), or 20 $\mu$M bovine serum albumin (▼). (In this case, the His tag was cleaved from the Ydj1.) *D*, fibril formation of 20 $\mu$M Ure2 alone (○) or in the presence of 20 $\mu$M Hdj1 (●) or 20 $\mu$M Hdj2 (▲). *E*, effect of delayed addition of Ydj1 during (*inset*) or after (*main panel*) the lag phase of Ure2 fibril formation. 30 $\mu$M Ure2 samples were incubated as in *A–D* but at reduced shaking intensity, and Ydj1 (●) or an equal volume of buffer (○) was added at the time point indicated (*arrow*). *AU*, arbitrary units.

protein (Fig. 3*C*). We also tested the effect of Ydj1 on Ure2 fibril formation under other conditions of temperature and shaking speed (see "Experimental Procedures"). A delay in the lag time of Ure2 fibril formation in the presence of Ydj1 was universally observed. However, the final plateau value varied with the reaction conditions; for a given chaperone ratio, a higher plateau was observed under conditions that disfavor amorphous aggregation (*e.g.* lower temperature, higher pH, lack of agitation). This is consistent with inhibition of fibril formation by a reversible interaction between Ure2 and Ydj1, coupled with competition between fibril formation and irreversible formation of amorphous aggregates (41).

In contrast to Ydj1, Hsp40-Sis1, which was unable to cure [*URE3*] (Fig. 1), showed no effect on the lag time of fibril formation of Ure2 under the same conditions (Fig. 3*C*). Similarly, the human Hsp40 homologues Hdj1 and Hdj2 showed no effect on Ure2 fibril formation under these conditions (Fig. 3*D*).

When the time of addition of Ydj1 was delayed until midexponential phase (data not shown), then no inhibition of fibril formation was observed. To investigate this further, we repeated the experiment at lower shaking intensity to slow the time course slightly and compared the addition of Ydj1 (or buffer) at $t = 0$, midlag time, and early exponential phase. As above, we found that Ydj1 had no effect when the addition was delayed until after the onset of the exponential phase (Fig. 3*E*, *main panel*), whereas the addition of Ydj1 within the lag time resulted in a significant delay in the onset of fibril formation (Fig. 3*E*, *inset*). This result suggests that the inhibitory effect of Ydj1 on fibril formation is due to interaction with the native state of Ure2 or an early intermediate in the fibril formation process.

*The Presence of Ydj1 Does Not Induce Significant Structural Change in Ure2*—The inhibition of Ure2 fibril formation by Ydj1 when added prior to the start of the exponential phase of fibril growth suggests a direct interaction between the proteins, possibly in their native states. We therefore used circular dichroism spectroscopy in the far-UV region (Fig. 4, *A* and *C*) and assay of Ure2 enzymatic activity (Fig. 4, *B* and *D*) to determine whether the interaction results in any significant change in the structure of the protein. As shown in Fig. 4*A*, the CD spectrum of an equimolar mixture of Ure2 and Ydj1 equaled that predicted from the simple addition of their individual spectra, suggesting that any interaction between the native states of Ure2 and Ydj1 does not result in any significant secondary structure change in either protein. The same result was observed for 90Ure2, which lacks the N-terminal prion-inducing domain (Fig. 4*C*). The presence of Ydj1 also had negligible

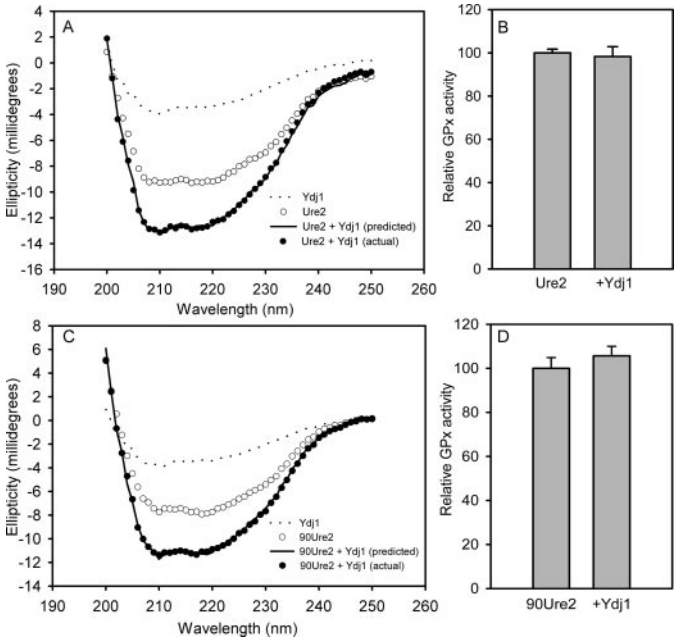


FIGURE 4. **Effect of the presence of Ydj1 on Ure2 structure and activity.** *A* and *C*, far-UV CD spectra of an equimolar mixture (●) of Ydj1 and Ure2 or 90Ure2, as indicated. Individual CD spectra of Ure2 (○) and Ydj1 (*dotted line*) were added to generate the predicted spectrum of the mixture (*solid line*). The buffer base line was subtracted from each data set. The spectra were measured at 37 °C in 50 mM Tris-HCl buffer, pH 7.5, containing 0.2 M NaCl after preincubation for 1 h. All protein concentrations were 20 μM. *B* and *D*, GPx activity of 30 μM native Ure2 or 90Ure2, as indicated, in the absence or presence of an equimolar concentration of Ydj1. The results shown are the mean of at least three independent measurements, and the *error bars* represent the S.E.

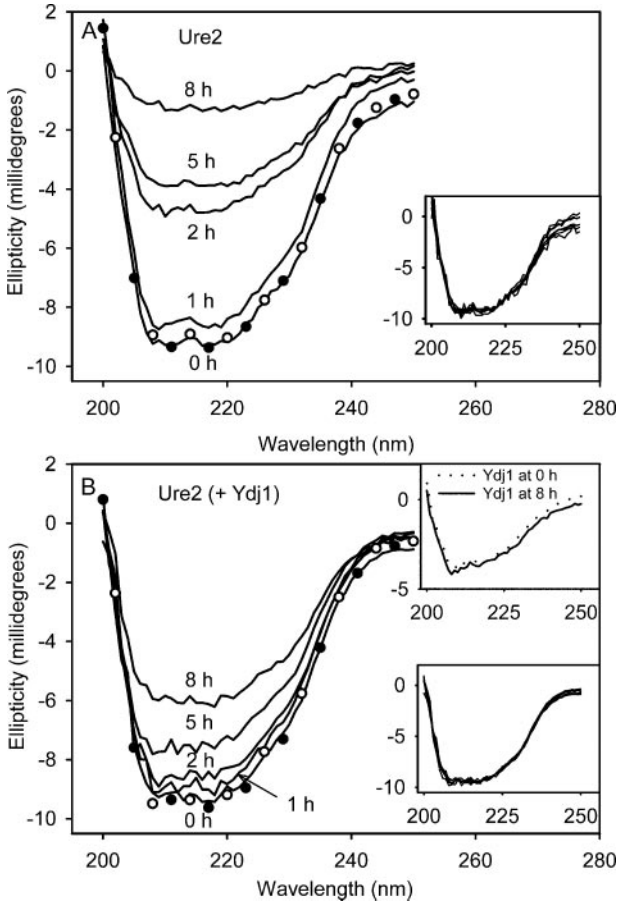


FIGURE 5. **Effect of Ydj1 on Ure2 secondary structure in soluble complexes formed during the lag time of fibril formation.** Incubation conditions were as described in the legend to Fig. 3. A series of samples were incubated in parallel, samples were removed at successive time points and centrifuged to remove large aggregates, and the supernatant was analyzed by far-UV CD. Time points corresponding to the lag time are 0 h, 15 min (○), 30 min (●), and 1 h. Time points from exponential or plateau phases (2, 5, and 8 h) are also shown. *A*, 20 μM Ure2 incubated alone. *Inset*, the same data as in the *main panel* normalized to the $t = 0$ value to allow the shape of the spectra to be compared. *B*, 20 μM Ure2 incubated in the presence of 20 μM Ydj1. The Ydj1 spectrum was subtracted in each case. *Upper inset*, the spectrum of Ydj1 incubated alone under the same conditions at the beginning and end of the time course. *Lower inset*, the same data as shown in the *main panel* were normalized to the $t = 0$ value to allow the shape of the spectra to be compared.

effect on the activity of native Ure2 (Fig. 4*B*) or 90Ure2 (Fig. 4*D*), indicating that the C-terminal GST-like region of Ure2 remains in a native conformation in the presence of Ydj1.

In order to investigate whether Ydj1 might form complexes with nonnative states of Ure2, particularly during the lag time of fibril formation, we also monitored the CD spectra of Ure2, in the presence and absence of Ydj1, throughout the time course of fibril formation (Fig. 5). The results confirm that Ydj1 does not alter the structure of Ure2 or stabilize partially folded intermediates but merely delays the process of fibril formation. This is consistent with a model where Ydj1 binds reversibly to the native state of Ure2.

*Ydj1 Interacts with the C-terminal Domain of Ure2, whereas Hdj2 Does Not*—In order to determine whether a direct interaction could be observed between Ure2 and Hsp40 chaperones, we performed size exclusion chromatography experiments. Due to the similarity in size between the 40-kDa protein Ure2 and the Hsp40 homologues Ydj1 (45 kDa), Hdj2 (45 kDa), Sis1 (38 kDa), and Hdj1 (38 kDa), the results of most size exclusion chromatography experiments were ambiguous as to the existence of an interaction, because the Ure2 and chaperone peaks overlapped. However, the elution times for the larger Type I homologues (*i.e.* Ydj1 or Hdj2) and that of N-terminally truncated Ure2 (*i.e.* 90Ure2 (30 kDa) or 105Ure2 (29 kDa)) were sufficiently well separated that the interaction could be studied. As shown in Fig. 6, the single peaks observed for Ydj1 and 105Ure2 were noticeably altered in the mixture, indicative of an interaction between the proteins. In contrast, no significant change was observed for 90Ure2 and Hdj2 (Fig. 6, *inset*). This result correlates with the inhibitory effect of Ydj1 on Ure2 fibril formation and the lack of effect of Hdj2. Further, it indicates that the N-terminal prion domain of Ure2 is not necessary for a stable interaction.

In order to investigate further the interaction between Ure2 and Ydj1, we measured SPR on a Biacore instrument. In this method, a ligand is immobilized on a gold surface modified with a dextran hydrogel layer, allowing the molecule to be maintained in its native state. The binding partner is then introduced as the analyte in the mobile phase that is perfused across the chip, allowing sensitive detection of interactions between molecules in real time. Ure2 or its mutant 90Ure2 were immobilized, and a gradient of concentrations of Ydj1 was perfused over the chip surfaces. On both the Ure2 and 90Ure2 chips, Ydj1 binding was concentration-dependent, and the association and dissociation phases could be observed clearly (Fig. 7, *A*

and *B*), indicating direct interaction of Ydj1 with both Ure2 and 90Ure2. When the binding of Ydj1 to Ure2 and to 90Ure2 was compared, both the association and dissociation phases showed slight differences (Fig. 7*C* and Table 1). Furthermore, the 90Ure2 chip was more difficult to be regenerated after Ydj1 binding. This could suggest that the N-terminal region of Ure2 influences the interaction between Ure2 and Ydj1. Alternatively, since WT and 90Ure2 were immobilized on the chips to give the same level of response (see "Experimental Procedures"), but the molecular weight of 90Ure2 is 25% lower than WT, the effective concentration of 90Ure2 on the chip may be higher. In any case, the fact that Ydj1 binds strongly not only to WT Ure2 but also to the N-terminally truncated mutant 90Ure2 indicates that it is mainly the C-terminal region of Ure2 that contributes to stable binding between Ydj1 and Ure2. To ensure that binding was specific, we included the nucleotide-dependent chaperone Hsp104 as a control. Under these conditions (*i.e.* in the absence of nucleotide), the control protein showed zero binding to immobilized WT Ure2 (Fig. 7*C*) or 90Ure2 (data not shown). The sensorgrams of Ydj1 binding to the Ure2 or 90Ure2 chips fit well to a bivalent analyte model, consistent with the dimeric state of Ydj1 (Fig. 7 and Table 1). The equilibrium dissociation constant for binding of Ydj1 to Ure2 could not be obtained from this experiment, since the rate constants obtained from the bivalent analyte model (Table 1) are not compatible with calculation of a meaningful value for $K_d$.

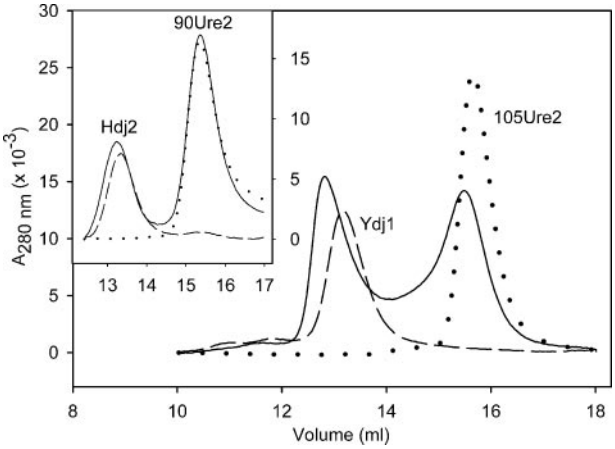


FIGURE 6. **Size exclusion chromatography analysis of interactions between N-terminally truncated Ure2 and Ydj1 or Hdj2.** Conditions were as follows: 50 mM Tris-HCl buffer, pH 7.5, containing 0.2 M NaCl at room temperature. Chromatograms for 105Ure2 (*dotted line*), Ydj1 (*dashed line*), and their 1:1 mixture (*solid line*). *Inset*, chromatograms for 90Ure2 (*dotted line*), Hdj2 (*dashed line*), and their 1:1 mixture (*solid line*).

In order to exclude the possibility that the preferential binding of Ydj1 to the globular C-terminal region of Ure2 was an artifact of immobilization of the protein, we performed a competitive binding experiment, by including WT Ure2 or the N-terminally truncated mutant 105Ure2 along with Ydj1 in the mobile phase and then monitoring binding to the Ure2 chip (Fig. 7*D*). The presence of a 15-fold excess of WT Ure2 in the mobile phase significantly reduced binding to immobilized Ure2, indicating that the interaction between Ydj1 and Ure2 also occurs in solution. This competition effect was at least as pronounced for 105Ure2 as for WT Ure2, confirming that Ydj1 interacts with the C-terminal globular domain of Ure2.

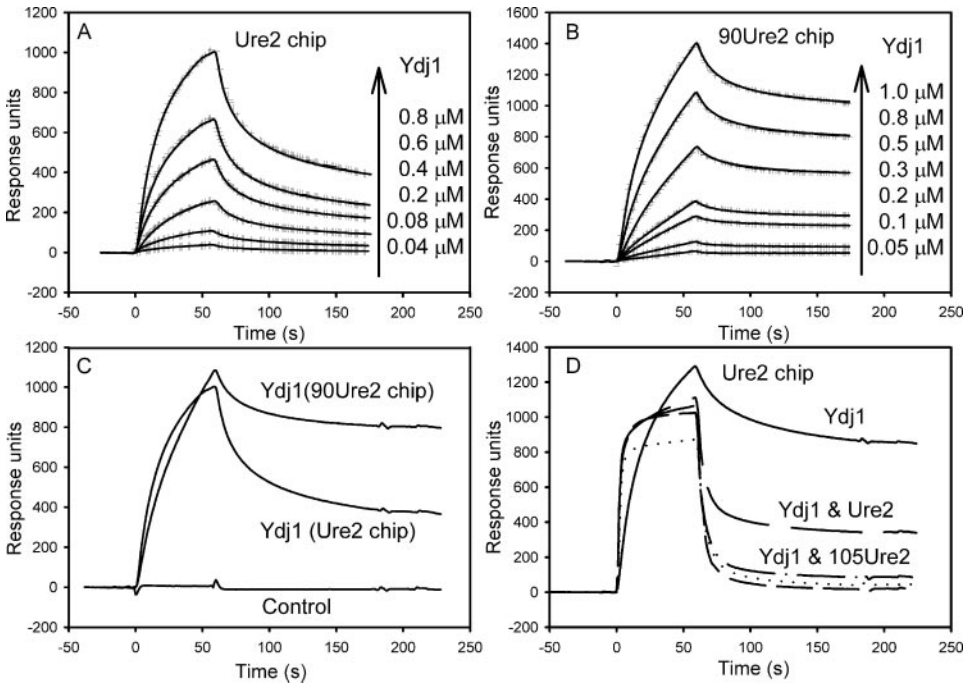


FIGURE 7. **Interaction of Ydj1 with Ure2 or N-terminally truncated Ure2 detected by SPR.** Different concentrations of Ydj1 were applied to chips containing immobilized Ure2 or 90Ure2. Conditions were as follows: 10 mM Hepes buffer, pH 7.4, containing 150 mM NaCl and 0.005% surfactant P20 at 25 °C. Composite Biacore sensorgrams show the binding responses (*solid lines*), which were fitted to a bivalent analyte model (*hatched lines*). The results of data fitting are shown in Table 1. *A*, binding of Ydj1 (injected mobile phase) to Ure2 (immobilized on the chip). The magnitude of the response increased with increasing Ydj1 concentration (as indicated). *B*, binding of Ydj1 to immobilized 90Ure2. The magnitude of the response increased with increasing Ydj1 concentration (as indicated). *C*, comparison of binding to immobilized Ure2 and 90Ure2. The concentration of Ydj1 in the injected mobile phase was 0.8 μM. As a control, the nucleotide-dependent chaperone Hsp104 (3.0 μM) showed zero binding to the Ure2 chip under the same conditions (*i.e.* in the absence of nucleotides). *D*, binding of Ydj1 (1.6 μM) to immobilized Ure2 in the presence and absence of a competing 15-fold excess of Ure2 or 105Ure2 in the mobile phase. High to low responses were as follows: Ydj1 alone, Ydj1 + WT Ure2, Ydj1 + 105Ure2, 105Ure2 alone, and WT Ure2 alone.

## DISCUSSION

Molecular chaperones play a crucial role in the cell by safeguarding proteins from misfolding and aggregation, particularly under conditions of stress, such as heat shock or disease (16, 17). In recent years, there has been increasing interest in diseases of protein misfolding and a concomitant emphasis on understanding how protein misfolding is controlled in the cell. There is mounting evidence that chaperones, particularly the Hsp70/Hsp40 system, may have therapeutic potential in misfolding diseases, such as

**TABLE 1**

**Apparent kinetic constants for binding of Ydj1 to immobilized Ure2 or 90Ure2**

The Biacore sensorgrams (Fig. 7) were fitted to a bivalent analyte model, to obtain the apparent kinetic constants shown. The data included in the fit were for Ydj1 concentrations between 0.2 and 1.0 $\mu$M. The values shown are the mean ± S.E. of the fit. A meaningful $K_d$ value cannot be calculated from the rate constants obtained from the bivalent analyte model.

| Immobilized protein | $k_{a1}$ | $k_{d1}$ | $k_{a2}$ | $k_{d2}$ |
|---|---|---|---|---|
| | $M^{-1}\,s^{-1}$ | $s^{-1}$ | $M^{-1}\,s^{-1}$ | $s^{-1}$ |
| WT Ure2 | $(9.1 \pm 1.3) \times 10^3$ | $(5.9 \pm 0.2) \times 10^{-2}$ | $(5.5 \pm 0.9) \times 10^{-6}$ | $(2.8 \pm 0.2) \times 10^{-3}$ |
| 90Ure2 | $(2.5 \pm 0.1) \times 10^3$ | $(8.3 \pm 0.4) \times 10^{-2}$ | $(3.4 \pm 0.1) \times 10^{-6}$ | $(7.9 \pm 0.2) \times 10^{-4}$ |

Alzheimer, Parkinson, and Huntington diseases and the prion diseases (51, 52). However, in order to harness the therapeutic potential of chaperones (or to mimic their properties with drugs) it is necessary to gain detailed insight into the mechanisms by which these molecules are able to recognize misfolded substrates and suppress their deleterious effects.

While Hsp40 acts as a co-chaperone to Hsp70 in a variety of cellular processes, it is thought that certain members of the Hsp40 family are also able to function as independent chaperones (15, 53). Genetic studies have identified a number of chaperones that modulate the behavior of yeast prions (21). Of particular pertinence to this study is that overexpression of Ydj1 cures [*URE3*] (22), as does overexpression of its Hsp70 partner Ssa1 (30). However, the mechanism of [*URE3*] curing by Ydj1 has not previously been investigated.

Here, we address this question by comparing the ability of a variety of Hsp70 co-chaperones to cure the [*URE3*] prion phenotype by overexpression *in vivo* (Fig. 1). Of a total of seven potential Hsp70 co-chaperones tested, including Hsp40 homologues Ydj1, Apj1, and Sis1, the tetratricopeptide repeat cofactors Cns1, Cpr7, and Sti1, and the Hsp70 nucleotide exchange factor Fes1, only Ydj1 could strongly impair propagation of [*URE3*] when overexpressed. Ydj1 and Sis1 are known to stimulate Hsp70 ATPase activity ~8–10-fold (19), and Sti1 and Cns1 have also been shown to dramatically stimulate the ATPase activity Hsp70 (54, 55). If Ydj1 were impairing [*URE3*] propagation by influencing the Hsp70-Ssa ATPase cycle, then we would expect to see similar effects by overexpression of Sti1 and Cns1 or any co-chaperone that influences the Hsp70 ATPase cycle in a way similar to Ydj1. This is not the case, suggesting that the curing effect of Ydj1 on [*URE3*] propagation may be independent of Hsp70.

In order to investigate whether the curing effect of Ydj1 toward [*URE3*] could be due to a direct chaperone-like effect on the Ure2 protein, we studied the interaction of the purified proteins *in vitro*. We found that Ydj1 suppresses amyloid-like fibril formation of Ure2, as detected by AFM imaging (Fig. 2) or by binding of the amyloid-specific dye ThT (Fig. 3). Under the same conditions, Sis1 was unable to inhibit Ure2 fibril formation. These results are consistent with the ability of Ydj1, but not Sis1, to cure [*URE3*]. The difference in effect on fibril formation between Ydj1 and Sis1 is also consistent with their different abilities in preventing aggregation (19, 20). Suppression of fibril formation and prevention of aggregation *in vitro* has been observed not only for Ydj1 but also for other Type I Hsp40s, such as bacterial DnaJ (53) and human Hdj2 (56). In contrast, the human type II Sis1 homologue, Hdj1, must cooperate with Hsp70 in order to suppress protein aggregation (38, 57). Although there is a clear structural difference between Type I and Type II Hsp40s, namely the absence of a zinc finger domain in the type II members, it is interesting that the Type I yeast Hsp40 homologue, Apj1, is unable to cure [*URE3*]. Similarly, the Type I human homologue Hdj2 does not interact with Ure2 or suppress its fibril formation *in vitro*, at least under the conditions studied here. The sequence identity between Ydj1 and Hdj2 is 47%, and identity between Ydj1 and Apj1 is 36%, although Apj1 contains some additional sequence regions not present in Ydj1 (see sequence alignment in Fig. S1). Thus subtle differences in chaperone structure and specificity may be crucial for recognition of Ure2 (and other yeast prion proteins) as substrates. The structural basis for this specificity is an interesting topic for further study and may provide insight into the mechanisms of prion propagation and its prevention.

We found that the extent of inhibition of Ure2 fibril formation increased as the molar concentration of Ydj1 was increased, implying that the mechanism of inhibition may involve a stable interaction between the proteins. Further, Ydj1 was only effective when added early in the process of fibril formation, indicating that Ydj1 interacts with native Ure2 or an early intermediate in the fibril formation process. We have previously carried out a detailed analysis of the time course of Ure2 fibril growth using ThT binding and AFM, under conditions similar to those used here (8). We observed a series of fibrillar intermediates that appeared in a time-dependent manner and varied in height (*i.e.* diameter) and morphology (*i.e.* twisted or smooth). Globular aggregates were also observed but did not appear to be obligate intermediates in the fibril assembly process (8). The thinnest fibrillar intermediates, whose appearance corresponds with the initial increase in ThT binding fluorescence, were found to adsorb only weakly to the mica surface of the AFM grid and therefore tended to be lost in the washing step of sample preparation. Thus, the earliest fibrillar intermediates are always underrepresented in the AFM experiments (8). This explains why the effect of Ydj1 on inhibition of fibril formation appears more marked in the AFM experiments (Fig. 2) than by ThT binding at the same molar ratio (Fig. 3). In the previous study, we also examined the effect of deletions in the N-terminal prion domain on the ability of Ure2 to form fibrils. Although the equivalent mutations all rendered Ure2 unable to induce the prion state *in vivo* (58, 59), the results we observed *in vitro* suggest that this is in fact a threshold effect (8). Mutants with large truncations in the prion domain (*e.g.* deletion of residues 1–41) were unable to form fibrils on the experimental time scale, whereas mutants with smaller truncations (*e.g.* residues 1–14) were able to form fibrils but with an increased lag time (8), similar to the effect of Ydj1. It seems that the addition of Ydj1, like N-terminal deletions, disfavors the nucleation process of Ure2 fibril formation. Thus, the observation of a

relatively modest increase in the lag time *in vitro* can represent the threshold required to prevent prion formation *in vivo*.

Ydj1, like its Hsp70 partners, is expected to recognize non-native polypeptides or partially folded intermediates (18–20). It was therefore somewhat unexpected to find that Ydj1 interacts equally well with WT Ure2 and the truncated mutants 90Ure2 or 105Ure2, in which the unstructured N-terminal prion domain is absent (Figs. 6 and 7). These results indicate that it is the C-terminal globular region of Ure2 that is principally responsible for stable binding to Ydj1, although this may of course facilitate interaction with the N-terminal domain. Comparison of circular dichroism spectra and assay of enzymatic activity showed that the C-terminal GST-like region of Ure2 maintains its native conformation in the presence of Ydj1 (Fig. 4). In the case of Ure2, the C-terminal GST-like region of Ure2 maintains its native conformation within fibrils (14). Monitoring of GPx activity during the course of fibril formation revealed that this is also true in the presence of Ydj1 (data not shown). Taken together, this implies that the interaction between Ydj1 and Ure2 involves recognition of a native substrate and may essentially rely on partitioning of Ure2 toward the soluble native dimeric state rather than recognition of misfolded states or aggregates *per se*. Similarly, the mechanism of inhibition of toxic aggregate formation by Hsp70/Hsp40 in the case of poly(Q) fragments of the Huntington disease-related protein, Huntingtin, is suggested to involve partitioning of native monomers (60). Stabilization of native states by binding of polypeptides or small molecules has been identified as an important strategy in prevention and treatment of protein misfolding diseases (51, 61–63). In the case of chaperone binding to Ure2, it is likely that steric hindrance plays a significant role in stabilizing the native dimer against formation of higher order oligomers and fibrils. Since the globular C-domain of Ure2 has successfully been crystallized (5, 10), the observation of a stable interaction between Ydj1 and the Ure2 C-terminal region makes this complex an interesting target for high resolution structural analysis.

The results presented here suggest that Ydj1 is able to act independently of its Hsp70 partners to inhibit prion-like aggregation of the yeast protein Ure2 and does so by direct interaction with the native state of Ure2. These findings highlight the potential of native state stabilization as a therapeutic strategy in controlling the process of protein misfolding and aggregation.

*Acknowledgments—We are grateful to Rick Morimoto (Northwestern University), Daniel Masison (National Institutes of Health), Mark Bycroft (Centre for Protein Engineering, Cambridge, UK), and Stefan Walter (Technical University of Munich) for providing plasmids and to Christophe Cullin (Bordeaux, France) for providing the [URE3] strain. We thank Dr. Xinyu Wang for assistance with the use of the Pistar instrument and Dr. Hui Li for assistance with AFM experiments.*

## REFERENCES


1. Wickner, R. B. (1994) *Science* **264,** 566–569
2. Masison, D. C., and Wickner, R. B. (1995) *Science* **270,** 93–95
3. Perrett, S., Freeman, S. J., Butler, P. J., and Fersht, A. R. (1999) *J. Mol. Biol.* **290,** 331–345
4. Thual, C., Komar, A. A., Bousset, L., Fernandez-Bellot, E., Cullin, C., and Melki, R. (1999) *J. Biol. Chem.* **274,** 13666–13674
5. Umland, T. C., Taylor, K. L., Rhee, S., Wickner, R. B., and Davies, D. R. (2001) *Proc. Natl. Acad. Sci. U. S. A.* **98,** 1459–1464
6. Taylor, K. L., Cheng, N., Williams, R. W., Steven, A. C., and Wickner, R. B. (1999) *Science* **283,** 1339–1343
7. Thual, C., Bousset, L., Komar, A. A., Walter, S., Buchner, J., Cullin, C., and Melki, R. (2001) *Biochemistry* **40,** 1764–1773
8. Jiang, Y., Li, H., Zhu, L., Zhou, J. M., and Perrett, S. (2004) *J. Biol. Chem.* **279,** 3361–3369
9. Lian, H. Y., Jiang, Y., Zhang, H., Jones, G. W., and Perrett, S. (2006) *Biochim. Biophys. Acta* **1764,** 535–545
10. Bousset, L., Belrhali, H., Janin, J., Melki, R., and Morera, S. (2001) *Structure* **9,** 39–46
11. Bousset, L., Belrhali, H., Melki, R., and Morera, S. (2001) *Biochemistry* **40,** 13564–13573
12. Cooper, T. G. (2002) *FEMS Microbiol. Rev.* **26,** 223–238
13. Coschigano, P. W., and Magasanik, B. (1991) *Mol. Cell. Biol.* **11,** 822–832
14. Bai, M., Zhou, J. M., and Perrett, S. (2004) *J. Biol. Chem.* **279,** 50025–50030
15. Walsh, P., Bursac, D., Law, Y. C., Cyr, D., and Lithgow, T. (2004) *EMBO Rep.* **5,** 567–571
16. Walter, S., and Buchner, J. (2002) *Angew. Chem. Int. Ed.* **41,** 1098–1113
17. Young, J. C., Agashe, V. R., Siegers, K., and Hartl, F. U. (2004) *Nat. Rev. Mol. Cell. Biol.* **5,** 781–791
18. Cyr, D. M. (1995) *FEBS Lett.* **359,** 129–132
19. Lu, Z., and Cyr, D. M. (1998) *J. Biol. Chem.* **273,** 27824–27830
20. Lu, Z., and Cyr, D. M. (1998) *J. Biol. Chem.* **273,** 5970–5978
21. Jones, G. W., and Tuite, M. F. (2005) *BioEssays* **27,** 823–832
22. Moriyama, H., Edskes, H. K., and Wickner, R. B. (2000) *Mol. Cell. Biol.* **20,** 8916–8922
23. Bradley, M. E., Edskes, H. K., Hong, J. Y., Wickner, R. B., and Liebman, S. W. (2002) *Proc. Natl. Acad. Sci. U. S. A.* **99,** Suppl. 4, 16392–16399
24. Gokhale, K. C., Newnam, G. P., Sherman, M. Y., and Chernoff, Y. O. (2005) *J. Biol. Chem.* **280,** 22809–22818
25. Lopez, N., Aron, R., and Craig, E. A. (2003) *Mol. Biol. Cell* **14,** 1172–1181
26. Sondheimer, N., Lopez, N., Craig, E. A., and Lindquist, S. (2001) *EMBO J.* **20,** 2435–2442
27. Kushnirov, V. V., Kryndushkin, D. S., Boguta, M., Smirnov, V. N., and Ter-Avanesyan, M. D. (2000) *Curr. Biol.* **10,** 1443–1446
28. Krzewska, J., and Melki, R. (2006) *EMBO J.* **25,** 822–833
29. Kryndushkin, D. S., Smirnov, V. N., Ter-Avanesyan, M. D., and Kushnirov, V. V. (2002) *J. Biol. Chem.* **277,** 23702–23708
30. Schwimmer, C., and Masison, D. C. (2002) *Mol. Cell. Biol.* **22,** 3590–3598
31. Roberts, B. T., Moriyama, H., and Wickner, R. B. (2004) *Yeast* **21,** 107–117
32. Loovers, H. M., Guinan, E., and Jones, G. W. (2007) *Genetics* **175,** 621–630
33. Cyr, D. M., Lu, X., and Douglas, M. G. (1992) *J. Biol. Chem.* **267,** 20927–20931
34. Glover, J. R., and Lindquist, S. (1998) *Cell* **94,** 73–82
35. Christianson, T. W., Sikorski, R. S., Dante, M., Shero, J. H., and Hieter, P. (1992) *Gene* (*Amst.*) **110,** 119–122
36. Miroux, B., and Walker, J. E. (1996) *J. Mol. Biol.* **260,** 289–298
37. Schirmer, E. C., Queitsch, C., Kowal, A. S., Parsell, D. A., and Lindquist, S. (1998) *J. Biol. Chem.* **273,** 15546–15552
38. Minami, Y., Hohfeld, J., Ohtsuka, K., and Hartl, F. U. (1996) *J. Biol. Chem.* **271,** 19617–19624
39. Terada, K., Kanazawa, M., Bukau, B., and Mori, M. (1997) *J. Cell Biol.* **139,** 1089–1095
40. Minami, Y., and Minami, M. (1999) *Genes Cells* **4,** 721–729
41. Zhu, L., Zhang, X. J., Wang, L. Y., Zhou, J. M., and Perrett, S. (2003) *J. Mol. Biol.* **328,** 235–254
42. Gill, S. C., and von Hippel, P. H. (1989) *Anal. Biochem.* **182,** 319–326
43. Galani, D., Fersht, A. R., and Perrett, S. (2002) *J. Mol. Biol.* **315,** 213–227
44. Silver, J. M., and Eaton, N. R. (1969) *Biochem. Biophys. Res. Commun.* **34,** 301–305
45. Bousset, L., Thomson, N. H., Radford, S. E., and Melki, R. (2002) *EMBO J.* **21,** 2903–2911

46. Catharino, S., Buchner, J., and Walter, S. (2005) *Biol. Chem.* **386,** 633–641
47. Naiki, H., Higuchi, K., Hosokawa, M., and Takeda, T. (1989) *Anal. Biochem.* **177,** 244–249
48. Nielsen, L., Khurana, R., Coats, A., Frokjaer, S., Brange, J., Vyas, S., Uversky, V. N., and Fink, A. L. (2001) *Biochemistry* **40,** 6036–6046
49. Schlumpberger, M., Wille, H., Baldwin, M. A., Butler, D. A., Herskowitz, I., and Prusiner, S. B. (2000) *Protein Sci.* **9,** 440–451
50. Ghaemmaghami, S., Huh, W. K., Bower, K., Howson, R. W., Belle, A., Dephoure, N., O'Shea, E. K., and Weissman, J. S. (2003) *Nature* **425,** 737–741
51. Muchowski, P. J., and Wacker, J. L. (2005) *Nat. Rev. Neurosci.* **6,** 11–22
52. Sakahira, H., Breuer, P., Hayer-Hartl, M. K., and Hartl, F. U. (2002) *Proc. Natl. Acad. Sci. U. S. A.* **99,** Suppl. 4, 16412–16418
53. Langer, T., Lu, C., Echols, H., Flanagan, J., Hayer, M. K., and Hartl, F. U. (1992) *Nature* **356,** 683–689
54. Hainzl, O., Wegele, H., Richter, K., and Buchner, J. (2004) *J. Biol. Chem.* **279,** 23267–23273
55. Wegele, H., Haslbeck, M., Reinstein, J., and Buchner, J. (2003) *J. Biol. Chem.* **278,** 25970–25976
56. Meacham, G. C., Lu, Z., King, S., Sorscher, E., Tousson, A., and Cyr, D. M. (1999) *EMBO J.* **18,** 1492–1505
57. Muchowski, P. J., Schaffar, G., Sittler, A., Wanker, E. E., Hayer-Hartl, M. K., and Hartl, F. U. (2000) *Proc. Natl. Acad. Sci. U. S. A.* **97,** 7841–7846
58. Edskes, H. K., Gray, V. T., and Wickner, R. B. (1999) *Proc. Natl. Acad. Sci. U. S. A.* **96,** 1498–1503
59. Edskes, H. K., and Wickner, R. B. (2002) *Proc. Natl. Acad. Sci. U. S. A.* **99,** Suppl. 4, 16384–16391
60. Wacker, J. L., Zareie, M. H., Fong, H., Sarikaya, M., and Muchowski, P. J. (2004) *Nat. Struct. Mol. Biol.* **11,** 1215–1222
61. Bullock, A. N., and Fersht, A. R. (2001) *Nat. Rev. Cancer* **1,** 68–76
62. Heiser, V., Scherzinger, E., Boeddrich, A., Nordhoff, E., Lurz, R., Schugardt, N., Lehrach, H., and Wanker, E. E. (2000) *Proc. Natl. Acad. Sci. U. S. A.* **97,** 6739–6744
63. Johnson, S. M., Wiseman, R. L., Sekijima, Y., Green, N. S., mski-Werner, S. L., and Kelly, J. W. (2005) *Acc. Chem. Res.* **38,** 911–921